Modeling and Experimental Validation of an EMS Demonstration Vehicle

No. 13
Thomas E Alberts
Professor, Dept. of Aerospace Engineering, Old Dominion University, Norfolk VA USA
talberts@odu.edu
Aravind Hanasoge
Doctoral Candidate, Dept. of Aerospace Engineering, Old Dominion University, Norfolk VA USA
ahanasog@.odu.edu

ABSTRACT: In this paper, Dynamic modeling, Numerical simulation and Experimental validation of an EMS demonstration vehicle is presented. The dynamic model incorporates rigid body modes as well as a finite number of flexible modes of vibration. Decentralized PD controllers are designed individually for each of the six electromagnets. These controllers are used in numerical simulation as well as in real time levitation of the vehicle. Comparison of levitation results between numerical simulation and real time data validated the dynamic model thus developed.

1 INTRODUCTION

A 5000 pound, EMS maglev demonstration system is currently being developed at Old Dominion University (ODU), Figure 1. As part of this on-going research, a linear structural model of the vehicle, along with the electrodynamics of the magnets was developed. Decentralized PD controllers for levitation control were designed based on the linear model. These controllers were used in real time levitation of the vehicle, and also in numerical simulation of the levitation using Matlab Simulink software. In this paper, development of the dynamic model, along with controller design is briefly discussed. Comparison between real time levitation data and numerical simulation data is presented. This comparison indicates the accuracy of the developed model and the effectiveness of the controllers in stabilizing the levitation.

2 EXPERIMENTAL SET-UP

The ODU Test Vehicle, shown in Figure 1, is a welded aluminum structure equipped with six Electromagnets, six Pulse Width Modulated (PWM) Power amplifiers, two linear induction motors (LIMs), along with position and acceleration sensors, data acquisition and control equipment. This structure is mounted on a segment of the track from ODU's 3600 foot Maglev guideway. This vehicle has been built to represent one of the two bogies underneath the Full-scale maglev vehicle at ODU. Current is sent into each of the six electromagnet coils through the PWM amplifiers. Six eddy-current based position sensors and six accelerometers are used to measure the vertical positions and vertical accelerations of the magnets respectively. An 8-pole butterworth anti-aliasing filter along with a digital low-pass filter is used to filter the noise in the signals. A National Instruments data acquisition card installed in a PC104-Plus computer is used for data acquisition and control. The data acquisition system is operated through Matlab/Simulink, using the xPC Target environment. Relevant system parameters are listed in Table 1. The sample rate is 10 kHz.

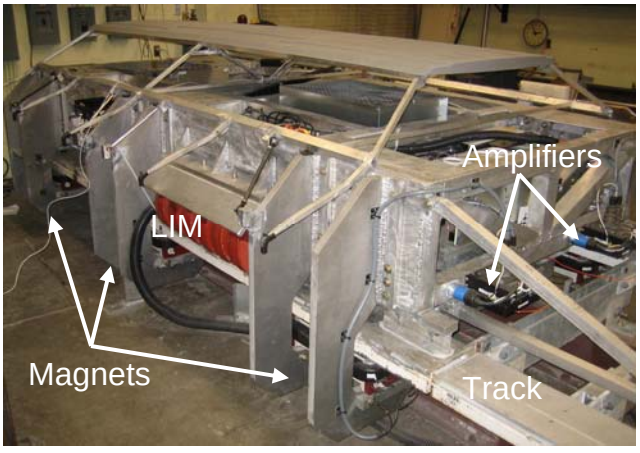

Figure 1 ODU Test vehicle in the laboratory.

Table 1. ODU Test Vehicle Parameters

Detail	Value	Units
Mass	2.267×10^3	kg
Length	3.65	m
Width	1.52	m
Height	0.91	m
Mass moment of Inertia (I_{xx})	2.955×10^3	kg.m^2
Mass moment of Inertia (I_{yy})	3.842×10^3	kg.m^2
Mass moment of Inertia (I_{zz})	1.207×10^3	kg.m^2
Desired Magnetic Gap	0.01	m
No. of Magnets	6	-
No. of Amplifiers	6	-
No. of LIMs	2	-
No. of Turns per magnet	596	-
Resistance of the magnet coil	1.83	Ω
Inductance of the magnet coil	0.68	H

3 MATHEMATICAL MODELING

3.1 Structural Model

The dynamic model of the vehicle includes rigid body and structural vibration modes. As a rigid body, it has 5 degrees of freedom – 2 in translation and 3 in rotation. Motion along the axis of propulsion is not modeled. As a flexible body (continuous system), it has infinite degrees of freedom (modes). However, here only few flexible modes are retained for the purposes of model development. The vehicle uses six electromagnets for levitation, and for the purposes of modeling the forces given by each magnet in both lateral and levitation directions are considered. The moments caused by these forces about the center of mass of the vehicle are also considered. A Finite Element (FE) structural model for the vehicle has been developed, from which the mass and inertia properties, basic geometry, location of the magnets with respect to the center of mass are obtained. Also obtained from the FE model are the mode shapes, (modal matrix or the matrix of eigenvectors) and eigenvalues (natural frequencies of vibration) of the vehicle for selected modes. The dynamics of a generic flexible structure with rigid body modes and a finite number of flexible modes of vibration can be modeled as [1]

$$A_s \ddot{\vec{p}} + B_s \dot{\vec{p}} + C_s \vec{p} = \Gamma^T \vec{u} \tag{1}$$

Where, A_s is the mass and inertia matrix given by

$$A_s = \begin{bmatrix} m_s & 0 & 0 \\ 0 & J_s & 0 \\ 0 & 0 & I_{n_q} \end{bmatrix} \tag{2}$$

m_s is the total mass of the structure times a 3×3 identity matrix (for translations along X, Y and Z directions), J_s is the 3×3 moment of inertia matrix, I_k denotes the $k\times k$ identity matrix, and n_q is the number of flexible modes of vibration retained.

$$\vec{p}^{\,T} = [\vec{x}_{rb}^{\,T} \quad \vec{q}_m^{\,T}]\,;\ \vec{x}_{rb} = [\vec{\xi}^{\,T} \quad \vec{\alpha}^{\,T}]^T \tag{3}$$

$\vec{\xi}$ and $\vec{\alpha}$ represent respectively, the rigid body translation and rigid body rotation vectors, $\vec{q}_m$ is the $n_q \times 1$ modal amplitude vector (modal co-ordinate vector).

$$B_s = \text{diag}[0_3 \quad 0_3 \quad D_{n_q\times n_q}] \tag{4a}$$

$$C_s = \text{diag}[0_3 \quad 0_3 \quad \Lambda_{n_q\times n_q}] \tag{4b}$$

Here D is the $n_q \times n_q$ symmetric matrix representing the inherent structural damping, and 0_k denotes the $k \times k$ null matrix, Λ is the diagonal matrix of squared elastic mode frequencies, and

$$\Gamma^T = \begin{bmatrix} I_3 & I_3 & \cdots & I_3 \\ \tilde{r}_1 & \tilde{r}_2 & \cdots & \tilde{r}_{m_f} \\ \Psi_1^T & \Psi_2^T & \cdots & \Psi_{m_f}^T \end{bmatrix} \tag{4c}$$

For the test vehicle, $m_f = 6$ is the number of applied forces, Ψ is the $3m_f \times n_q$ mode shape matrix, $\tilde{r}_i$ represents a 3 × 3 skew symmetric matrix that serves as a cross product operator for the position vector of the i^{th} force applying actuator. This means, for example, that the moment caused by the i^{th} force $\vec{f}_i$ about the center of gravity of the vehicle can be written as

$$\vec{M}_i = \vec{r}_i \times \vec{f}_i = \tilde{r}_i \vec{f}_i^{\,T} \tag{4d}$$

where $\vec{r}_i$ is the position vector for the i^{th} force applying actuator and $\vec{M}_i$ is the corresponding moment vector.

u is the input vector of applied forces, given by

$$u = \begin{bmatrix} \vec{f}_1^{\,T} & \vec{f}_2^{\,T} & \cdots & \vec{f}_{m_f}^{\,T} \end{bmatrix}^T \tag{5}$$

Considering the translational and rotational displacements and their rates at the sensor locations as the outputs, it is seen that the output vector is given by

$$\vec{y}_p = \Gamma \vec{p} \tag{6}$$

3.2 State-Space Model

Defining the states as the rigid body and flexible displacements and velocities, the state vector is constructed as

$$\vec{X} = \begin{bmatrix} \vec{x}_{rb}^T & \vec{q}_m^T & \dot{\vec{x}}_{rb}^T & \dot{\vec{q}}_m^T \end{bmatrix}^T \tag{7a}$$

The state-space model, therefore can be cast as follows:

$$\begin{aligned} \dot{\vec{X}} &= A\vec{X} + B\vec{u} \\ \vec{Y} &= C\vec{X} \end{aligned} \tag{7b}$$

where $\vec{u}$ and $\vec{Y}$ are given in Eqs (5) and (6) respectively, and

$$A = \begin{bmatrix} A_R & 0 \\ 0 & A_F \end{bmatrix} \qquad A_R = \begin{bmatrix} 0 & 0 & I & 0 \\ 0 & 0 & 0 & I \\ 0 & 0 & 0 & 0 \\ 0 & 0 & 0 & 0 \end{bmatrix} \tag{7c}$$

$$A_F = \begin{bmatrix} 0 & I \\ -\Lambda & -D \end{bmatrix}$$

$$B = \begin{bmatrix} B_R \\ B_F \end{bmatrix} \qquad B_R = \begin{bmatrix} 0 & 0 & 0 & 0 \\ 0 & 0 & 0 & 0 \\ m_s^{-1} & m_s^{-1} & \cdots & m_s^{-1} \\ J_s^{-1}\tilde{r}_1 & J_s^{-1}\tilde{r}_2 & \cdots & J_s^{-1}\tilde{r}_{m_f} \end{bmatrix} \tag{7d}$$

$$B_F = \begin{bmatrix} 0 & 0 & 0 & 0 \\ \Psi_1^T & \Psi_2^T & \cdots & \Psi_{m_f}^T \end{bmatrix}$$

The rows and columns of the *A* matrix are selected from the general *A* matrix given in Eq. 7c, depending on the desired degrees of freedom to be modeled. Depending on the desired force inputs (levitation only, lateral only, or both) to the vehicle, the corresponding columns of the *B* matrix should be selected. Similarly, depending on the desired outputs of the model (levitation gaps only, lateral offsets only or both) the corresponding rows of the *C* matrix are selected.

Using the FE model, one can obtain the mass and inertial properties of the structure, the natural frequencies of vibration (eigenvalues) and the mode shapes (eigenvectors). Node numbers corresponding to the magnet and sensor positions are used to obtain the input-output dynamics of the vehicle in terms of transfer functions. The frequency response corresponding to the colocated transfer function for each input/output pair of the vehicle structure as obtained from the FE model is shown in Figure 2. These are the transfer functions for the force input to position output at each magnet location.

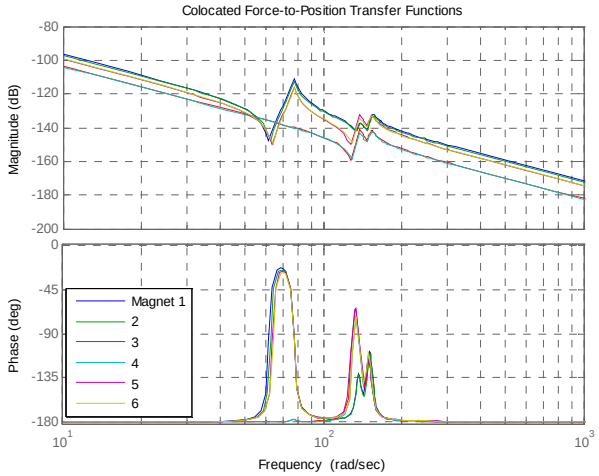

Figure 2 Colocated Structural Transfer Functions: Force to Position

3.3 Electrodynamics

The Electromagnetic levitation force is known to depend on the current supplied and the magnetic gap. This relationship which is non-linear, depends on the configurations of the magnet core and the track. For the configuration of the magnets on the ODU test vehicle, an appropriate levitation force expression for the i^{th} electromagnet (assuming zero lateral offset) is [3], [4]

$$f_{li} = \frac{1}{4}\frac{\mu_0 N^2 I_i^2 dw}{z_i^2}\left\{1 + \frac{2z_i}{\pi w}\right\} \tag{8}$$

In the above expression, z_i and I_i represent the gap and current at the i^{th} electromagnet. μ_0, d, N, w represent respectively permeability of air, length of the magnet core, number of turns in the coil and the width of the magnet core. Similarly, the inductance of the i^{th} coil can be expressed as

$$L_i = \frac{1}{2}\mu_0 dN^2\left[-\frac{w}{2z_i} - \frac{1}{\pi}\ln\left(\frac{1}{z_i}\right)\right] \tag{9}$$

The non-linear expression for force in Eq. (8) is linearized about the operating point (z_0, I_0). This linearized equation can be written as

$$f_{li} \cong k_I I_i - k_z z_i \tag{10a}$$

Where:

$$k_I = \frac{1}{2}\frac{\mu_0 N^2 dw I_0}{z_0^2}\left(1 + 2\frac{z_0}{\pi w}\right) \tag{10b}$$

$$k_z = \frac{1}{2}\frac{\mu_0 N^2 dw {I_0}^2}{{z_0}^3}\left(1+2\frac{z_0}{\pi w}\right)-\frac{\mu_0 N^2 d {I_0}^2}{2\pi {z_0}^2} \quad (10c)$$

Electromagnets are driven by PWM power (current) amplifiers, and these amplifiers follow a current command I^c with a current feedback gain K_a. With this, the governing equation for the i^{th} electromagnetic circuit can be written as

$$\dot{I}_i = I_i^c \beta_i - I_i \alpha_i + r\dot{z}_i \quad (11a)$$

Where:

$$\alpha_i = \frac{K_a + R}{L(z_i)}; \beta_i = \frac{K_a}{L(z_i)}; r = \frac{k_z}{k_I} \quad (11b)$$

3.4 A complete Linear Model

To incorporate the electrodynamics into the dynamic model of the vehicle, define the new state vector as

$$\tilde{\vec{X}} = \begin{bmatrix} \vec{X}^T & \vec{I}^T \end{bmatrix}^T \quad (12a)$$

Where $\vec{X}$ is as given in Eq. (7a), and

$$\vec{I} = \begin{bmatrix} I_1 & I_2 & \cdots & I_6 \end{bmatrix} \quad (12b)$$

Therefore, the new state-space model can be written as

$$\begin{aligned} \dot{\tilde{\vec{X}}} &= \tilde{A}\tilde{\vec{X}} + \tilde{B}\tilde{\vec{u}} \\ \tilde{\vec{Y}} &= \tilde{C}\tilde{\vec{X}} \end{aligned} \quad (13)$$

The input vector will now be

$$\tilde{\vec{u}} = \begin{bmatrix} I_1^c & I_2^c & \cdots & I_6^c \end{bmatrix}^T \quad (14)$$

The parameters can be arranged in matrices as follows:

$$K_z = diag(k_z \quad k_z \quad \cdots \quad k_z) \quad (15a)$$

$$K_I = diag(k_I \quad k_I \quad \cdots \quad k_I) \quad (15b)$$

$$\rho = diag(r \quad r \quad \cdots \quad r) \Rightarrow \rho K_I = K_z \quad (15c)$$

$$\alpha = diag(\alpha_1 \quad \alpha_2 \quad \cdots \quad \alpha_6) \quad (15d)$$

$$\beta = diag(\beta_1 \quad \beta_2 \quad \cdots \quad \beta_6) \quad (15e)$$

With this the state-space parameter matrices become:

$$\tilde{A} = \begin{bmatrix} A - BK_z C & BK_I \\ \rho C(A - BK_z C) & \rho CBK_I - \alpha \end{bmatrix} \quad (16a)$$

$$\tilde{B} = \begin{bmatrix} 0 \\ \beta \end{bmatrix}; \tilde{C} = \begin{bmatrix} C & 0 \end{bmatrix} \quad (16b)$$

Colocated transfer functions between current input and position output for each magnet are shown in terms of frequency response in Figure 3.

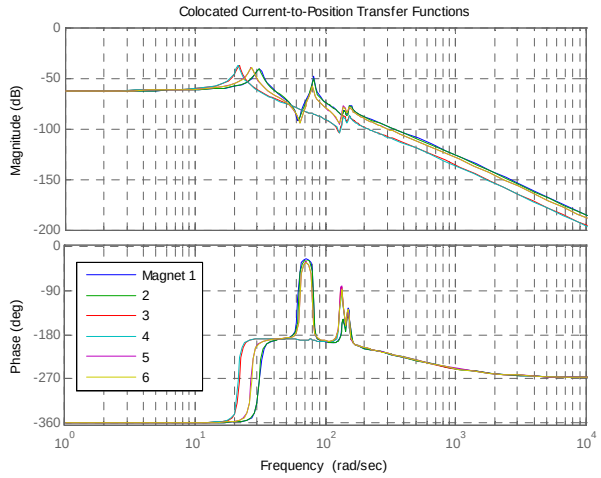

Figure 3 Colocated Transfer Functions: Current to Position

4 CONTROLLER DESIGN AND SIMULATION

4.1 Controller Design

A Decentralized PD controller is designed for each of the six magnets, based on the linear dynamic model given in Eqs. (13) – (16). These controllers are independently designed using Matlab. As an example, the root locus of the system with input levitation force on Magnet #1 and the output as the levitation gap of Magnet #1 is shown in Figure 4. The corresponding PD controller used is:

$$C(s) = K_p + K_d s \quad (17)$$

These controllers are implemented in real-time levitation of the vehicle, and are fine-tuned for better performance based on the experimental results. In practice a slow integrator term is added to reduce steady state error.

4.2 Numerical Simulation

Numerical simulation of the closed-loop non-linear dynamics of the vehicle is carried out using Simulink. A schematic illustrating the simulation scheme is shown in Figure 5. The controllers used for the simulation are the same as the ones used in the real time experiments.

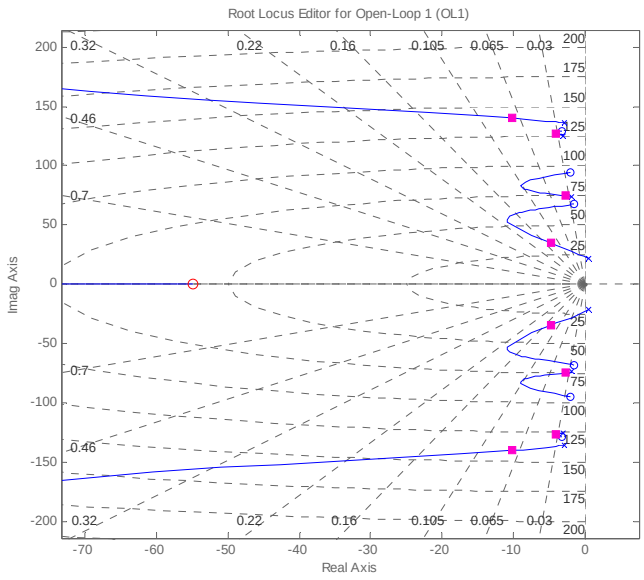

Figure 4 Root Locus for Typical PD Control Loop

The simulation model is implemented in discrete time, since the real time data acquisition and control is in discrete time. A finite number of flexible modes are included in the simulation. The results presented here include 4 vibration modes.

5 RESULTS

Figures 6 and 7 show the comparison between experimentally obtained data and simulation data. The vehicle was levitated using the four corner magnets, which are designated as magnets 1, 2, 5 and 6. Magnetic gaps at each of the four magnets, and the current input to the magnets are shown. From these results, it can be seen that the simulated dynamics closely match the dynamics of the physical system.

6 CONCLUSIONS

This paper has presented a dynamic model for a maglev test vehicle under development at Old Dominion University. Experiments have been conducted which serve to validate the model. The model, which includes rigid body and flexible modes, can be used to evaluate stability, ride quality and disturbance response characteristics of the vehicle. Since stability of maglev systems with structural flexibility is of particular interest, future plans include the incorporation of a model for guideway flexibility.

7 REFERENCES

1. Joshi, S. M. Control of Large Flexible Structures, Lecture notes in Control and Informational Sciences, Springer-Verlag, 1989
2. Sinha, K., "Electromagnetic Suspension-Dynamics & Control", Peter Peregrinus, London, 1987
3. Limbert, A., Richardson, H.H. & Wormley, D.N. 1976. "Controlled Dynamic Characteristics of Ferromagnetic Vehicle Suspension Providing Simultaneous Lift and Guidance. Journal of Dynamics systems, Measurement and control 101:217:222
4. Alberts, T.E., Oleszczuk, G., and Hanasoge, A.M., "Stable Levitation Control of Magnetically Suspended Vehicles with Structural Flexibility", Proceedings of the 2008 American Control Conference, pp. 4035-4040
5. Hanasoge, A.M., Omran, A.F., Alberts, T.E., "Model Validation of a Magnetic Ball Levitation System" Proceedings of the ASME Dynamic Systems and Control Conference, To Appear, 2008

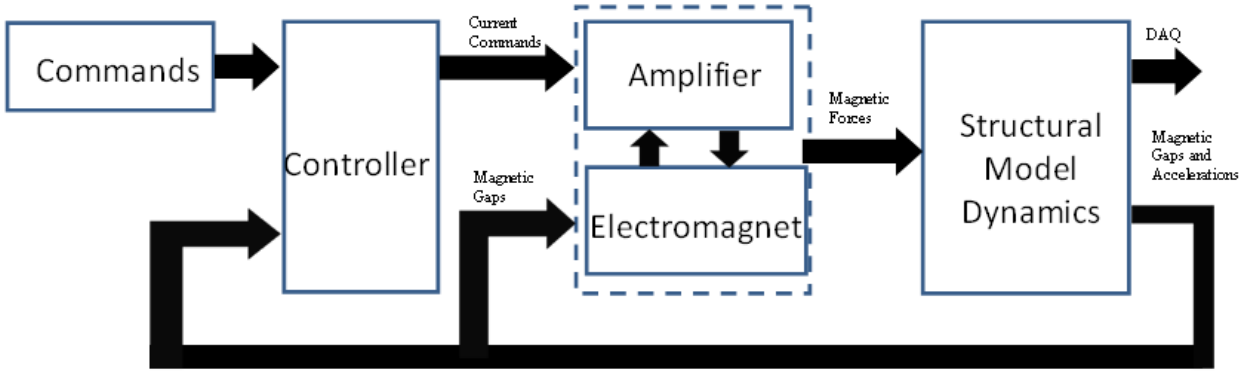

Figure 5. Simulation Block Diagram

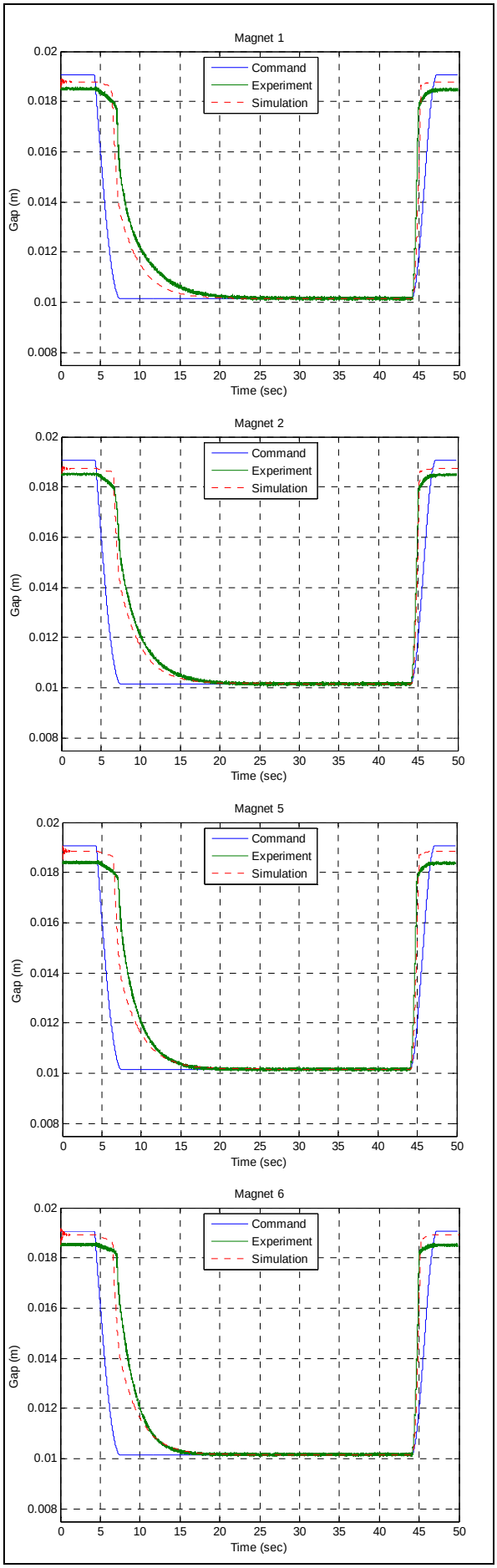

Figure 6 Gap Response Comparison

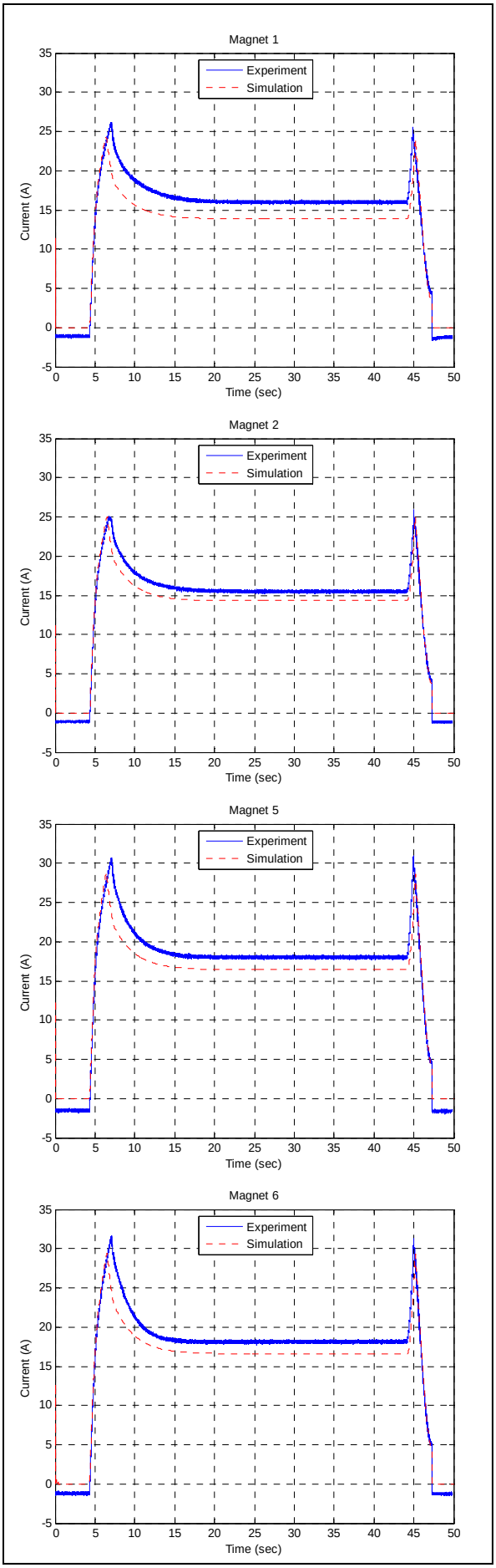

Figure 7 Input Current Comparison